Phylogenetic analysis

Phylogenies were analysed using PAUP* v4.0b10 (ref. 26), PAML v3.14 (ref. 27) and MrBayes v3.0b4 (ref. 28). To determine the best-fit likelihood model for nucleotide data, hierarchical likelihood ratio tests were performed on 100 randomly selected alignments chosen from experimental data sets (using Modelltest v3.06 (ref. 29), $\alpha = 0.05$). The true JC69 model was strongly supported and was used for all maximum likelihood and BMCMC DNA analyses. The true Poisson model was used for protein analysis, and maximum parsimony used equal weights. We performed likelihood-based analyses with and without gamma and invariant sites models to determine their effect on accuracy. The covarion model implemented in MrBayes was also used. Topology searches were exhaustive for maximum parsimony and maximum likelihood. BMCMC analysis involved four chains (three heated) run well past stationarity.

To determine support, we used nonparametric bootstrapping (1,000 replicates) for maximum parsimony and maximum likelihood and posterior probability for BMCMC, with a support cutoff value of 95% to construct strongly supported consensus trees. (See Supplementary Information for details on phylogenetic methods.)

Accuracy

The accuracy of each method was calculated as the proportion of replicates for which the correct topology was uniquely recovered (ϕ). Nonlinear regression was performed using the logistic equation $\phi = 1/(1 + \exp((BL_{50} - r)H))$, in which BL_{50} is the estimated internal branch length that produces 50% correct recovery, and H estimates the steepness of the performance curve. The significance of differences among BL_{50}s was examined by a t-test.

Bias and error

The type I error rate for each method was determined by analysing data sets generated under strong heterotachy with zero-length internal branches and determining the fraction of replicates falsely resolved with 95% bootstrap or posterior probability support[30]. The presence of bias was determined by calculating the proportion of erroneous estimates consistent with each possible incorrect topology over all internal branch lengths. The intensity of bias was investigated by calculating the proportion of erroneous topology estimates consistent with each possible incorrect topology when a 95% support cutoff was imposed.

To determine the impact of homogeneous optimization of branch lengths on maximum likelihood error, we compared the standard maximum likelihood algorithm that estimates a single set of branch lengths (ML_{homo}) with several partitioned maximum likelihood models with constrained branch lengths. ML_{true} constrains all branch lengths for each site to the true values used to simulate data sets. ML_{term} constrains the internal branch lengths to the true value for each site, but terminal branches have the lengths homogeneously optimized under ML_{homo}. ML_{short} assumes the true internal and long terminal branches but uses the short terminal length from ML_{homo}. ML_{long} constrains the internal and short terminal branches to their true values and takes the long terminal branch length from ML_{homo}.

Support for the true topology by each character-state pattern was calculated from a 100,000-site data set constructed under strong heterotachy ($p = 0.75$, $q = 0.05$, $r = 0.254$). Net support for the true tree is defined as the likelihood ratio of the true tree to the incorrect tree for each pattern x, weighted by the frequency of x ($f(x)$) in the data set: $S_{((AB),(CD)),x} = \frac{P(x|((AB),(CD)))}{P(x|((AC),(BD)))} f(x)$.

To determine the performance impact of violating the identical distribution assumption when the true evolutionary model is used, we implemented a novel likelihood model ($BMCMC_{hetero}$) that incorporates heterotachy a posteriori by applying two sets of branch lengths to the data. For each sequence site x_i, the likelihood of tree t with branch length sets b_1 and b_2 is $L(t|x_i) = \sum_{j=1}^{2} [\rho_{i,j} \cdot P(x_i|t, b_j)]$, where $\rho_{i,j}$—the posterior probability that x_i is in branch length set b_j—is calculated from the data as $\rho_{i,j} = P(x_i|t, b_j)/\sum_{k=1}^{2} P(x_i|t, b_k)$. The overall posterior probability of each topology is calculated using BMCMC (see Supplementary Information). This new method was compared with a BMCMC analysis using the true heterogeneous model and correct a priori data partitioning ($BMCMC_{true}$).

Received 17 May; accepted 6 August 2004; doi:10.1038/nature02917.

1. Sanderson, M. J. & Kim, J. Parametric phylogenetics? *Syst. Biol.* **49,** 817–829 (2000).
2. Hillis, D. M., Huelsenbeck, J. P. & Cunningham, C. W. Application and accuracy of molecular phylogenies. *Science* **264,** 671–677 (1994).
3. Felsenstein, J. Cases in which parsimony and compatibility methods will be positively misleading. *Syst. Zool.* **27,** 401–410 (1978).
4. Kuhner, M. K. & Felsenstein, J. A simulation comparison of phylogeny algorithms under equal and unequal evolutionary rates. *Mol. Biol. Evol.* **11,** 459–468 (1994).
5. Huelsenbeck, J. P. Systematic bias in phylogenetic analysis: is the Strepsiptera problem solved? *Syst. Biol.* **47,** 519–537 (1998).
6. Gaut, B. S. & Lewis, P. O. Success of maximum likelihood phylogeny inference in the four-taxon case. *Mol. Biol. Evol.* **12,** 152–162 (1995).
7. Huelsenbeck, J. P. Testing a covariotide model of DNA substitution. *Mol. Biol. Evol.* **19,** 698–707 (2002).
8. Miyamoto, M. M. & Fitch, W. M. Testing the covarion hypothesis of molecular evolution. *Mol. Biol. Evol.* **12,** 503–513 (1995).
9. Lopez, P., Casane, D. & Philippe, H. Heterotachy, an important process of protein evolution. *Mol. Biol. Evol.* **19,** 1–7 (2002).
10. Fitch, W. M. The molecular evolution of cytochrome c in eukaryotes. *J. Mol. Evol.* **8,** 13–40 (1976).
11. Pollock, D. D., Taylor, W. R. & Goldman, N. Coevolving protein residues: maximum likelihood identification and relationship to structure. *J. Mol. Biol.* **287,** 187–198 (1999).
12. Pupko, T. & Galtier, N. A covarion-based method for detecting molecular adaptation: application to the evolution of primate mitochondrial genomes. *Proc. R. Soc. Lond. B* **269,** 1313–1316 (2002).
13. Inagaki, Y., Susko, E., Fast, N. M. & Roger, A. J. Covarion shifts cause a long-branch attraction artifact that unites Microsporidia and Archaebacteria in EF-1{alpha} phylogenies. *Mol. Biol. Evol.* **21,** 1340–1349 (2004).
14. Lockhart, P. J. *et al.* A covariotide model explains apparent phylogenetic structure of oxygenic photosynthetic lineages. *Mol. Biol. Evol.* **15,** 1183–1188 (1998).
15. Misof, B. *et al.* An empirical analysis of mt 16S rRNA covarion-like evolution in insects: site-specific rate variation is clustered and frequently detected. *J. Mol. Evol.* **55,** 460–469 (2002).
16. Philippe, H. & Lopez, P. On the conservation of protein sequences in evolution. *Trends Biochem. Sci.* **26,** 414–416 (2001).
17. Donaldson, T. S. Robustness of the F-test to errors of both kinds and the correlation between the numerator and denominator of the F-ratio. *J. Am. Stat. Assoc.* **63,** 660–676 (1968).
18. Sullivan, J. & Swofford, D. L. Should we use model-based methods for phylogenetic inference when we know that assumptions about among-site rate variation and nucleotide substitution pattern are violated? *Syst. Biol.* **50,** 723–729 (2001).
19. Hillis, D. M. Taxonomic sampling, phylogenetic accuracy, and investigator bias. *Syst. Biol.* **47,** 3–8 (1998).
20. Chang, J. T. Inconsistency of evolutionary tree topology reconstruction methods when substitution rates vary across characters. *Math. Biosci.* **134,** 189–215 (1996).
21. Rokas, A., Williams, B. L., King, N. & Carroll, S. B. Genome-scale approaches to resolving incongruence in molecular phylogenies. *Nature* **425,** 798–804 (2003).
22. Russo, C. A., Takezaki, N. & Nei, M. Efficiencies of different genes and different tree-building methods in recovering a known vertebrate phylogeny. *Mol. Biol. Evol.* **13,** 525–536 (1996).
23. Delarbre, C., Gallut, C., Barriel, V., Janvier, P. & Gachelin, G. Complete mitochondrial DNA of the hagfish, *Eptatretus burgeri*: the comparative analysis of mitochondrial DNA sequences strongly supports the cyclostome monophyly. *Mol. Phylogenet. Evol.* **22,** 184–192 (2002).
24. Naylor, G. J. & Brown, W. M. Amphioxus mitochondrial DNA, chordate phylogeny, and the limits of inference based on comparisons of sequences. *Syst. Biol.* **47,** 61–76 (1998).
25. Tuffley, C. & Steel, M. Links between maximum likelihood and maximum parsimony under a simple model of site substitution. *Bull. Math. Biol.* **59,** 581–607 (1997).
26. Swofford, D. L. *PAUP*: Phylogenetic Analysis Using Parsimony and Other Methods, v.4.0b10* (Sinauer Associates, Sunderland, Massachusetts, 1998).
27. Yang, Z. PAML: a program package for phylogenetic analysis by maximum likelihood. *Comput. Appl. Biosci.* **13,** 555–556 (1997).
28. Huelsenbeck, J. P. & Ronquist, F. MRBAYES: Bayesian inference of phylogenetic trees. *Bioinformatics* **17,** 754–755 (2001).
29. Posada, D. & Crandall, K. A. MODELTEST: testing the model of DNA substitution. *Bioinformatics* **14,** 817–818 (1998).
30. Swofford, D. L. *et al.* Bias in phylogenetic estimation and its relevance to the choice between parsimony and likelihood methods. *Syst. Biol.* **50,** 525–539 (2001).

Supplementary Information accompanies the paper on **www.nature.com/nature**.

Acknowledgements We thank J. Conery for advice, support and programming advice. P. Phillips, R. DeSalle and S. Proulx provided comments and discussion. We benefited from discussions of mixed model methods with D. Zwickl. B.K. was supported by an NSF IGERT training grant in Evolution, Development and Genomics to the University of Oregon.

Competing interests statement The authors declare that they have no competing financial interests.

Correspondence and requests for materials should be addressed to J.T. (joet@uoregon.edu).

Ecological constraints on diversification in a model adaptive radiation

Rees Kassen[1,2], Martin Llewellyn[1]* & Paul B. Rainey[1,3]

[1]*Department of Plant Sciences, University of Oxford, South Parks Road, Oxford OX1 3RB, UK*
[2]*Department of Biology & Centre for Advanced Research in Environmental Genomics, University of Ottawa, Ottawa K1N 6N5, Canada*
[3]*School of Biological Sciences, University of Auckland, Private Bag 92019, Auckland, New Zealand*

* Present address: London School of Hygiene and Tropical Medicine, Keppel Street, London WC1E 7HT, UK

Taxonomic diversification commonly occurs through adaptive radiation, the rapid evolution of a single lineage into a range of genotypes or species each adapted to a different ecological niche[1,2]. Radiation size (measured as the number of new types) varies widely between phylogenetically distinct taxa[2–4] and between replicate radiations within a single taxon where the ecological opportunities available seem to be identical[5,6]. Here we

show how variation in energy input (productivity) and environmental disturbance combine to determine the extent of diversification in a single radiating lineage of *Pseudomonas fluorescens* adapting to laboratory conditions. Diversity peaked at intermediate rates of both productivity and disturbance and declined towards the extremes in a manner reminiscent of well-known ecological patterns[7–9]. The mechanism responsible for the decrease in diversity arises from pleiotropic fitness costs associated with niche specialization[10,11], the effects of which are modulated by gradients of productivity and disturbance. Our results indicate that ecological gradients may constrain the size of adaptive radiations, even in the presence of the strong diversifying selection associated with ecological opportunity, by decoupling evolutionary diversification from ecological coexistence.

The size of an adaptive radiation is thought to be governed by the extent of ecological opportunity (defined as the number of vacant niches or unutilized resources; where 'niches' refers to the collection of sites within an environment offering different conditions of growth) in a given geographical region or community[1,2,12]. This requires the processes of evolutionary diversification (which introduces variant types into the community) and ecological assortment (which can eliminate new types) to be closely matched. Any factor that influences the relative rates at which these two processes occur is likely to have an impact on the size of a given adaptive radiation such that diversification may be less (or more) extensive than predicted on the basis of ecological opportunity alone. Relevant factors include contingent or idiosyncratic increases in the probability of diversification or extinction through sexual selection[13], drift[7] or loss of habitat associated with decreasing area[14]. A more general factor may arise from pleiotropic fitness costs associated with niche specialization, particularly if the magnitude of the cost is affected by ecological conditions[2,3,15].

To understand the effect of ecological constraints on diversification we allowed replicate populations of a single genotype of the soil bacterium *P. fluorescens* SBW25 to diversify in spatially structured (static) microcosms across gradients of productivity and disturbance over the course of 16 days in the absence of predation. Ecological opportunity is afforded by the combination of spatial structure of the microcosms and resource depletion in the broth caused by the growth and metabolism of the ancestral population. Under these conditions, *P. fluorescens* rapidly diversifies into niche specialist genotypes that differ in colony morphology on agar plates and occupy different ecological regions of a static microcosm[11]. The diversity in these communities is non-neutral, being stably maintained by negative frequency-dependent selection, and the extent of diversification has been shown to be related to nutrient concentration[16]. When spatial structure is removed by shaking, diversification of the kind observed in the presence of spatial structure does not occur and diversity is rapidly lost from previously diverse cultures[11,17,18].

Figures 1 and 2 depict the response of diversity and richness (number of morphotypes) to gradients of both productivity and disturbance after 16 days. There is a peak at intermediate rates of both, a result confirmed by an analysis of covariance showing a significant negative quadratic relationship between diversity and both productivity and disturbance but no significant linear relationship (Table 1). This bivariate pattern of diversity is also consistent with purely ecological models of competition between niche specialists under resource competition[8,19–21] and in the presence of coarse-grained spatial heterogeneity[17,18,22,23] (see Supplementary Information). Note, however, that as interpretations of our data these models are not appropriate because they do not account for diversification from an initially isogenic state.

The two dominant niche specialists in our experiment were the ancestral smooth, which occupies the broth, and wrinkly spreader, which colonizes the air–broth interface. Note that a single smooth morphotype dominates at the extremes of both productivity and disturbance (Fig. 2a, e). We did observe other types (including the fuzzy spreader morph that inhabits the bottom of the microcosm and many variant types within categories), however these never comprised more than 5% of the total population so we do not consider them further.

These results are consistent with previous work, which has highlighted the importance of spatial structure[11,17,18] and resource competition[11,16,24] for the emergence and maintenance of diversity; the results are also consistent with our knowledge of the evolutionary ecology of *P. fluorescens* in static microcosms. In spatially structured microcosms the key limiting resource seems to be oxygen. Shallow oxygen gradients arise even in the absence of bacteria, owing to diffusion and the special properties of liquid surfaces. These gradients are steepened by the metabolic activities of growing bacteria, causing intense resource competition that drives diversification. This interpretation is consistent with the ecological theory of adaptive radiation[2,15] that sees diversification being spurred initially by divergent natural selection underlain by environmental heterogeneity and subsequently driven by resource competition.

Mutation in the ancestral smooth population constantly introduces new variants into the population where, under standard conditions (intermediate nutrient concentrations and disturbance frequencies), strong diversifying selection favours the evolution of niche specialist genotypes—one of the most successful being the wrinkly spreader which, by overproducing an adhesive polymer[25], can grow at the air–liquid interface where oxygen is abundant. Diversity is maintained through negative frequency-dependent selection generated through the combination of resource competition and spatial structure. Under frequent disturbances and low nutrient concentrations, population sizes are large enough (approximately 2×10^7 cells ml^{-1}) to guarantee a constant supply of new mutants, including wrinkly spreader, but not to permit formation of a coherent mat, which requires expression of an energetically costly adhesive cellulosic polymer[10,24,25]. At high nutrient concentrations and infrequent disturbances, intense resource

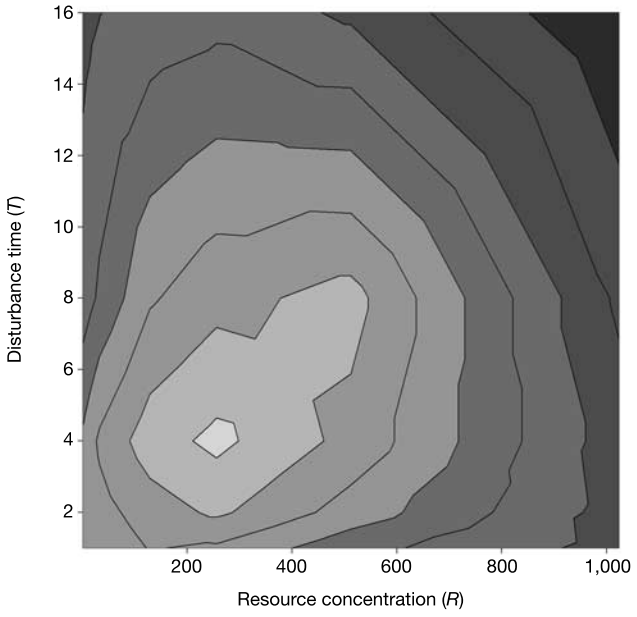

Figure 1 The joint effect of productivity and disturbance on diversity, as $1 - \lambda$, for the experiment. Data were transformed by Loess smoothing using a sampling proportion of 0.5. High diversity regions are shown in lighter shades, low diversity regions in darker shades. Values of diversity may be read directly from the graphs in Fig. 2.

competition leads to strong diversifying selection and the evolution of a thick wrinkly spreader mat. Eventually the mat sinks under its own weight. The collapse is further hastened by smooth morphotypes that act as cheats by invading the mat, thereby gaining access to oxygen, but contributing nothing towards mat strength[24].

The overproduction of cellulose characteristic of wrinkly spreader is accompanied by a pleiotropic fitness cost[10], the precise effects of which appear to be dependent on the ecological gradients of productivity and disturbance. Experimental evidence supporting this interpretation is shown in Fig. 3, which depicts the population density of smooth and wrinkly spreader genotypes as pure cultures and in competitive mixtures over 4 days across five levels of productivity. The population density of the smooth morphotypes is typically 1–2 orders of magnitude higher than wrinkly spreader after 1 day of growth in both pure and mixed cultures, reflecting the inability of wrinkly spreader to form a coherent mat in overnight cultures and implying that the smooth morphotype is the superior competitor under frequent disturbances. On day two and after, the wrinkly spreader morphotype typically achieves population densities comparable to that of smooth in pure culture (Fig. 3a–e) across the entire range of productivities, but is inferior to smooth at low ($0.00781\times$, $0.125\times$) and high ($8\times$) resource supply rates (Fig. 3f, g, j). After 4 days of growth at the highest productivity level ($8\times$), the density of smooth is moderately but significantly greater when cultured in the presence of wrinkly spreader than in its absence (one-tailed t-test: $t = 4.64$; $P = 0.005$, degrees of freedom $= 2$; compare Fig. 3e, j), whereas that of wrinkly spreader is again lower when competing against smooth (Fig. 3e, j). This result is consistent with the idea that the smooth genotype gains a fitness advantage at the air–broth interface, hastening the collapse of the mat[24].

The reduced competitive ability of wrinkly spreader relative to smooth at the extremes of productivity and disturbance could arise through changes in either the relative fitness of either type in

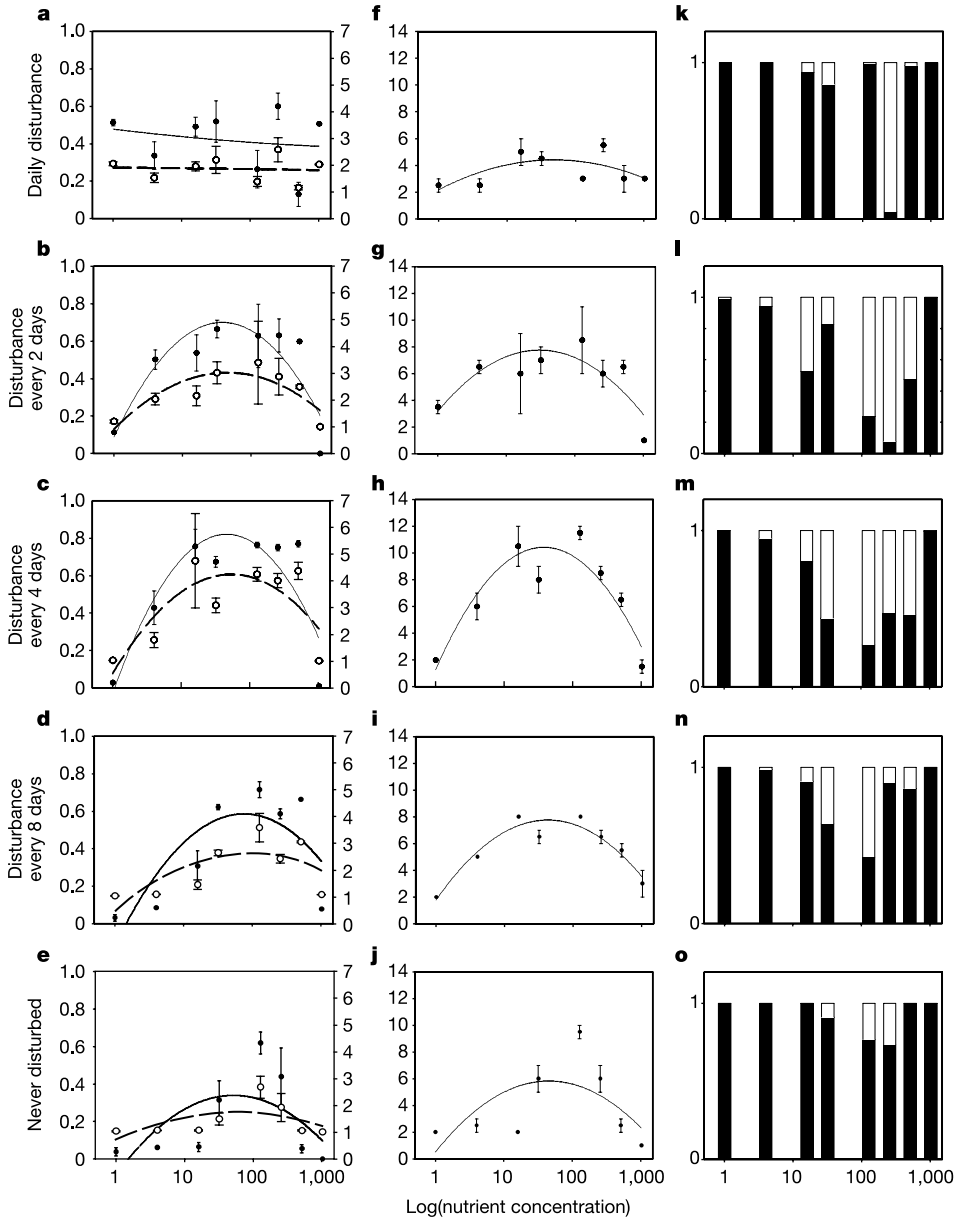

Figure 2 Diversity in relation to productivity, according to disturbance regime. **a**–**e**, Diversity expressed as $1 - \lambda$ (solid line) and $1/\lambda$ (dashed line) (± 1 standard error). **f**–**j**, Diversity expressed as richness; that is, the number of distinct colony morphs (± 1 standard error). **k**–**o**, The frequency of smooth morphotypes (filled sections) relative to the frequency of all other types, at each level of productivity.

Table 1 **Analysis of covariance for the experiment**

Source	Degrees of freedom	Mean square	*F* statistic	*P*-value	Parameter estimate (±standard error)	Partial r^2
Productivity						
Linear	1	0.138	3.38	0.070	0.35 ± 0.19	0.06
Quadratic	1	0.533	13.1	0.001	−0.15 ± 0.04	0.26
Disturbance						
Linear	1	0.023	0.57	0.451	0.42 ± 0.55	0.07
Quadratic	1	0.164	4.03	0.048	−0.62 ± 0.31	0.07
Productivity x disturbance						
Linear	1	0.076	1.88	0.175	–	–
Quadratic	1	0.028	0.70	0.406	–	–
Residual	71	0.041	–	–	–	–

The dependent variable is diversity, measured as the complement of Simpson's index. Performing the same analysis using the reciprocal of Simpson's index gives comparable results.

competition or through the total production of individuals (carrying capacity) associated with a given patch or resources[19,23,26,27]. The results depicted in Fig. 3 allow us to distinguish between these alternatives. If differences in competitive ability arise through changes in carrying capacities alone, then the population densities of the two types in pure culture should diverge through time, with smooth becoming more abundant than wrinkly spreader. Our results do not support this prediction (Fig. 3a–e), suggesting that the competitive superiority of smooth across a gradient of productivity stems from changes in the relative fitness of wrinkly spreader associated with the overproduction of cellulose rather than through changes to the relative carrying capacities of the two types.

Given the large population sizes (over 7×10^6 cells ml^{-1}) and asexual nature of reproduction in these populations, genetic drift and hybridization among incipient niche specialists can be eliminated as explanations for the variance in diversity observed in our experiment. An alternative explanation is that the extent of ecological opportunity, and so the strength of diversifying selection promoting diversification, decreases at the extremes of productivity and disturbance. A similar mechanism has been used to explain ecological patterns of diversity along productivity gradients in plant communities[28], and it may account for the inability of wrinkly spreader to invade a population of smooth morphotypes from rare at low productivity and under frequent disturbance (mean fitness ± 95% confidence limits of a standard laboratory genotype of wrinkly spreader after 1 day of competition against SBW25 at 0.00781 × normal resource concentration and introduced at a ratio by volume of 1:100: 1.15 ± 1.11). However, wrinkly spreader is capable of invading from rare a smooth morphotype population under infrequent disturbance regimes[18] and at high productivities in overnight competitions (mean fitness ± 95% confidence limits as above at 8 × normal resource concentration: 1.86 ± 0.27), suggesting that the ecological opportunity conferred through the combination of smooth morphotype population growth and spatial structure persists when disturbance is rare and productivity high.

Ecological gradients of productivity and disturbance may thus constrain the equilibrium level of diversity achieved after adaptive radiation by decoupling evolutionary diversification from ecological coexistence, rather than through changes to the extent of ecological opportunity. The cause of this decoupling in the *P. fluorescens* radiation stems from the pleiotropic costs of niche specialization[10] and manifests as costs of adaptation associated with resource competition in a spatially structured environment. This mechanism may provide a simple explanation for the variation in size between replicate adaptive radiations: large and spectacular radiations imply the existence of abundant ecological opportunity but are likely to be rare because the conditions promoting diversification may be different from those ensuring its maintenance. It is interesting to note that the pattern of species diversity in at least two well-known replicate radiations—among islands in the Hawaiian *Tetragnatha* spiders[29] and the Galapagos finches (see Supplementary Fig. 2)—is unimodal, peaking on islands of intermediate age, in a manner reminiscent of our results. It is tempting to interpret these patterns along similar lines, although a variety of other factors such as dispersal[3], sexual selection[13], loss of habitable area[14] or population

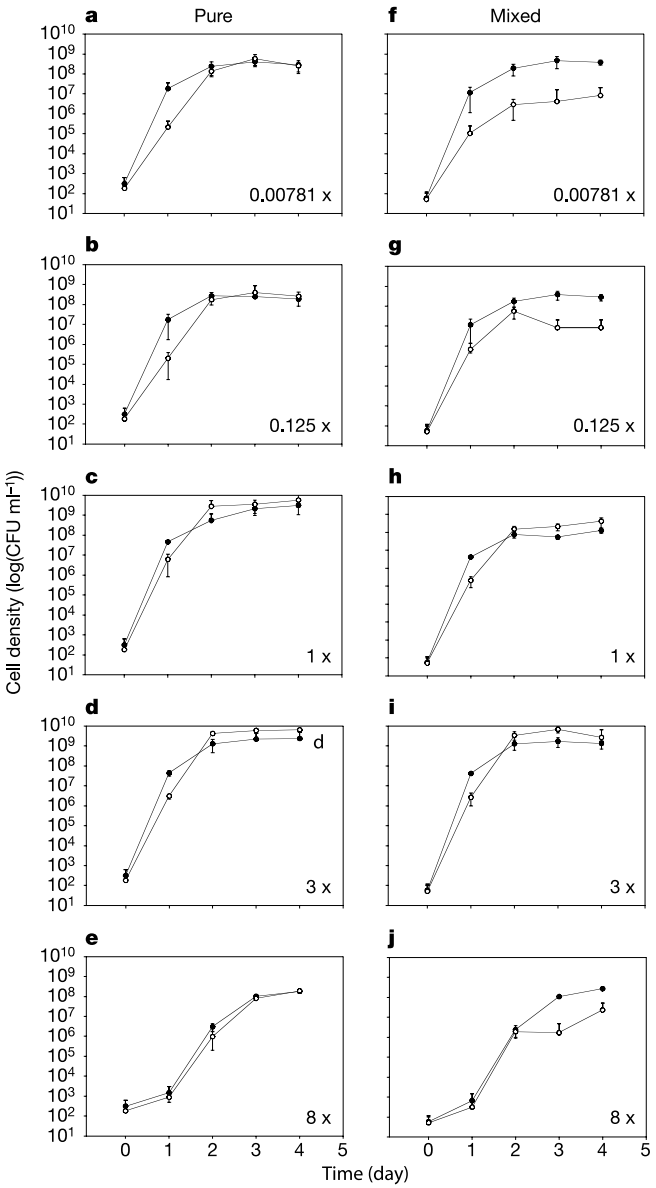

Figure 3 Population density (log(CFU ml^{-1})) of smooth (filled circles) and wrinkly spreader (open circles) morphotypes over 4 days across a productivity gradient. **a**–**e**, Pure culture. **f**–**j**, Mixed culture. Error bars are 95% confidence limits.

persistence[7] may further contribute to the variance in species diversity between replicate radiations in these more complex systems. Nevertheless our results, taken together with those of a recent study demonstrating that a further cost of adaptation may be to limit diversification itself[30], provides strong support for the importance of constraints in governing the size of adaptive radiations. □

Methods

Diversification across productivity and disturbance gradients

Following previous work[17,18], a gradient of productivity was constructed through serial dilution of a standard growth medium across a threefold range of nutrient concentrations from 8 × to 0.00758 × normal for a total of eight productivity levels. Global disturbances were imposed by transferring a 6-μl aliquot (approximately 10^7 cells) from a microcosm that had been vigorously vortexed for approximately 45 s to obtain a completely mixed population into 6 ml of fresh medium daily, every 2 days, every 4 days, every 8 days, or not at all, over the course of 16 days. Cultures were plated and scored for the frequency of different colony morphologies at the end of the experiment. Diversity was estimated as the complement and reciprocal of Simpson's index, $1 - \lambda$ and $1/\lambda$, respectively, where $\lambda = \Sigma p_i^2$ and p_i is the frequency of each colony type counted from approximately 100 colonies and used in all statistical analyses. Final population sizes varied between 7×10^6 to 2×10^9 cells ml^{-1}, making sampling effects an unlikely explanation for our results. Note that the disturbance regime allows for approximately ten generations of growth per transfer, so frequently disturbed populations will have undergone more selection than less frequently disturbed populations. This provides a likely explanation for the high diversity at the extreme productivity levels under the daily transfer regime (Fig. 1), which was due to the presence of different kinds of smooth genotypes (Fig. 2a, f, k).

Despite obvious and dense growth in the microcosms at 8 × standard nutrient concentration in the never-transferred disturbance regime, we were unable to obtain viable cells on plates from fresh cultures. Viable cells were present in the culture, however, as aliquots from frozen samples grew when inoculated into fresh medium. To estimate diversity, we allowed frozen samples of cells to recover in standard concentrations of liquid King's B medium for approximately 7 h before plating. We observed only smooth colony morphotypes from these recovered populations. Data from these cultures are treated as missing values in the statistical analysis but have been included in Figs 1 and 2 for clarity.

Population density in pure and mixed cultures

Pure and mixed cultures of the ancestral smooth (SBW25) and a derived wrinkly spreader genotype were inoculated at low density ($n \pm$ s.e.m; smooth 311 ± 58; wrinkly spreader 180 ± 51) into static microcosms at five productivity levels (0.00781×, 0.125×, 1×, 3× and 8× standard). Three replicates of each genotype and mixture were grown at 28 °C and destructively sampled every day for 4 days. We measured the population size of both genotypes by counting the number of colony-forming units (CFU) at known dilution in four 10-μl drops on standard KB agar plates.

Received 17 September; accepted 6 August 2004; doi:10.1038/nature02923.

1. Simpson, G. G. *The Major Features of Evolution* (Columbia Univ. Press, New York, 1953).
2. Schluter, D. *The Ecology of Adaptive Radiation* (Oxford Univ. Press, Oxford, 2000).
3. Givnish, T. J. in *Molecular Evolution and Adaptive Radiation* (eds Givnish, T. J. & Sytsma, K. J.) 1–54 (Cambridge Univ. Press, Cambridge, 1997).
4. Conway Morris, S. in *Evolution of Biological Diversity* (eds Magurran, A. E. & May, R. M.) 283–321 (Oxford Univ. Press, Oxford, 1999).
5. Meyer, A. Phylogenetic relationships and evolutionary processes in East African cichlid fishes. *Trends Ecol. Evol.* **8,** 267–305 (1993).
6. Williams, E. E. The origin of faunas—evolution of lizard congeners in a complex island fauna: a trail analysis. *Evol. Biol.* **6,** 47–89 (1972).
7. Rosenzweig, M. L. *Species Diversity in Space and Time* (Cambridge Univ. Press, Cambridge, 1995).
8. Huston, M. A. *Biological Diversity* (Cambridge Univ. Press, Cambridge, 1994).
9. Connell, J. H. Diversity in tropical rainforests and coral reefs. *Science* **199,** 1302–1310 (1978).
10. Maclean, R. C., Bell, G. & Rainey, P. B. The evolution of a pleiotropic fitness trade-off in *Pseudomonas fluorescens*. *Proc. Natl Acad. Sci. USA* **101,** 8072–8077 (2004).
11. Rainey, P. B. & Travisano, M. Adaptive radiation in a heterogeneous environment. *Nature* **394,** 69–72 (1998).
12. Day, T. & Young, K. A. Competitive and facilitative evolutionary diversification. *Bioscience* **54,** 101–109 (2004).
13. Seehausen, O., van Alphen, J. J. M. & Witt, F. Cichlid fish diversity threatened by eutrophication that curbs sexual selection. *Science* **277,** 1808–1811 (1997).
14. Losos, J. B. & Schluter, D. Analysis of an evolutionary species-area relationship. *Nature* **408,** 847–850 (2000).
15. Doebeli, M. & Dieckmann, U. Speciation along environmental gradients. *Nature* **421,** 259–264 (2003).
16. Travisano, M. & Rainey, P. B. Studies of adaptive radiation using microbial model systems. *Am. Nat.* **156,** S35–S44 (2000).
17. Kassen, R. *et al.* Diversity peaks at intermediate productivity in a laboratory microcosm. *Nature* **406,** 508–512 (2000).
18. Buckling, A. *et al.* Disturbance and diversity in experimental microcosms. *Nature* **408,** 961–964 (2000).
19. Riebesell, J. F. Paradox of enrichment in competitive systems. *Ecology* **55,** 183–187 (1974).
20. Kondoh, M. Unifying the relationships of species richness to productivity and disturbance. *Proc. R. Soc. Lond. B* **268,** 269–271 (2001).
21. Worm, B. *et al.* Consumer versus resource control of species diversity and ecosystem functioning. *Nature* **417,** 848–851 (2002).
22. Levene, H. Genetic equilibrium when more than one niche is available. *Am. Nat.* **87,** 331–333 (1953).
23. Maynard Smith, J. & Hoekstra, R. Polymorphism in a varied environment: how robust are the models? *Genet. Res.* **35,** 45–57 (1980).
24. Rainey, P. B. & Rainey, K. Evolution of cooperation and conflict in experimental populations of bacteria. *Nature* **425,** 72–74 (2003).
25. Spiers, A. J. *et al.* Biofilm formation at the air-liquid interface by the *Pseudomonas fluorescens* SBW25 wrinkly spreader requires an acetylated form of cellulose. *Mol. Microbiol.* **50,** 15–27 (2003).
26. Holt, R. D. Adaptive evolution in source-sink environments: direct and indirect effects of density-dependence on niche evolution. *Oikos* **75,** 182–192 (1996).
27. Kawecki, T. J., Barton, N. H. & Fry, J. D. Mutational collapse of fitness in marginal habitats and the evolution of ecological specialization. *J. Evol. Biol.* **10,** 407–429 (1997).
28. Tilman, D. *Resource Competition and Community Structure* (Princeton Univ. Press, Princeton, 1982).
29. Gillespie, R. Community assembly through adaptive radiation in Hawaiian spiders. *Science* **303,** 356–359 (2004).
30. Buckling, A., Wills, M. A. & Colegrave, N. Adaptation limits diversification of experimental bacterial populations. *Science* **302,** 2107–2109 (2003).

Supplementary Information accompanies the paper on **www.nature.com/nature**.

Acknowledgements We thank G. Bell, T. Day, M. Doebeli, B. Kerr, J. Pannell and D. Schluter for critical reviews of the manuscript and discussion. A. Gunn and J. Stansfield provided technical assistance. This work was supported by grants from NSERC (Canada) and St Hugh's College, Oxford, to R.K. and BBSRC (UK) and NERC (UK) to P.B.R.

Competing interests statement The authors declare that they have no competing financial interests.

Correspondence and requests for materials should be addressed to R.K. (rkassen@uottawa.ca).

Megabase deletions of gene deserts result in viable mice

Marcelo A. Nóbrega*, Yiwen Zhu*, Ingrid Plajzer-Frick, Veena Afzal & Edward M. Rubin

DOE Joint Genome Institute Walnut Creek, California 94598, USA, and Genomics Division Lawrence Berkeley National Laboratory Berkeley, California 94720, USA

* These authors contributed equally to this work

The functional importance of the roughly 98% of mammalian genomes not corresponding to protein coding sequences remains largely undetermined[1]. Here we show that some large-scale deletions of the non-coding DNA referred to as gene deserts[2–4] can be well tolerated by an organism. We deleted two large non-coding intervals, 1,511 kilobases and 845 kilobases in length, from the mouse genome. Viable mice homozygous for the deletions were generated and were indistinguishable from wild-type littermates with regard to morphology, reproductive fitness, growth, longevity and a variety of parameters assaying general homeostasis. Further detailed analysis of the expression of multiple genes bracketing the deletions revealed only minor expression differences in homozygous deletion and wild-type mice. Together, the two deleted segments harbour 1,243 non-coding sequences conserved between humans and rodents (more than 100 base pairs, 70% identity). Some of the deleted sequences might encode for functions unidentified in our screen; nonetheless, these studies further support the existence of potentially 'disposable DNA' in the genomes of mammals.

The genome of an organism is frequently referred to as its 'book of life'[5]. It remains unclear, however, whether this is an information-dense book, in which every page is required for the proper telling of the story, or whether some of it is disposable, without an impact on the story line. For coding regions, the general necessity of maintaining most genes in animal genomes has been established in many studies. Although gene inactivation can sometimes fail to result in

ERRATUM

doi:10.1038/nature03683

Reduction of hysteresis losses in the magnetic refrigerant $Gd_5Ge_2Si_2$ by the addition of iron

Virgil Provenzano, Alexander J. Shapiro & Robert D. Shull

Nature **429**, 853–857 (2004)

The date of acceptance of this Letter was 17 May 2004, and not 5 December 2004 as published.

ERRATUM

doi:10.1038/nature03684

Ecological constraints on diversification in a model adaptive radiation

Rees Kassen, Martin Llewellyn & Paul B. Rainey

Nature **431**, 984–988 (2004)

This Letter was submitted on 17 September 2003 and accepted on 9 August 2004; the dates are incorrect as published.

ERRATUM

doi:10.1038/nature03621

Foreshock sequences and short-term earthquake predictability on East Pacific Rise transform faults

Jeffrey J. McGuire, Margaret S. Boettcher & Thomas H. Jordan

Nature **434**, 457–461 (2005)

This Article was accepted for publication on 19 January 2005, and not on 19 December 2005 as published.

CORRIGENDUM

doi:10.1038/nature03656

A universal trend of amino acid gain and loss in protein evolution

I. King Jordan, Fyodor A. Kondrashov, Ivan A. Adzhubei, Yuri I. Wolf, Eugene V. Koonin, Alexey S. Kondrashov & Shamil Sunyaev

Nature **433**, 633–638 (2005)

We reported a universal trend of amino-acid gain and loss observed for recent evolutionary history among a diverse set of 15 taxa, with amino acids of declining frequencies being the first to be incorporated into the genetic code and those of increasing frequencies being late recruits. We have since discovered that a similar scenario for protein evolution was proposed by Zuckerkandl and colleagues more than thirty years ago[1]. Their analysis of a far smaller vertebrate-specific data set of two protein families also revealed asymmetric patterns of amino-acid substitution, and they went on to speculate that "extrapolation to zero occurrence of the rare amino acids might define the time at which they were introduced into the genetic code."

1. Zuckerkandl, E., Derancourt, J. & Vogel, H. Mutational trends and random processes in the evolution of informational macromolecules. *J. Mol. Biol.* **59**, 473–490 (1971).

CORRIGENDUM

doi:10.1038/nature03655

Low dose oral cannabinoid therapy reduces progression of atherosclerosis in mice

Sabine Steffens, Niels R. Veillard, Claire Arnaud, Graziano Pelli, Fabienne Burger, Christian Staub, Meliha Karsak, Andreas Zimmer, Jean-Louis Frossard & François Mach

Nature **434**, 782–786 (2005)

Meliha Karsak was accidentally omitted from the author list of this Letter; she has the same affiliation as A.Z.